Maxwell's demon and quantum-dot cellular automata

John Timler and Craig S. Lent[a)]
Department of Electrical Engineering, University of Notre Dame, Notre Dame, Indiana 46556

(Received 6 January 2003; accepted 18 April 2003)

Quantum-dot cellular automata (QCA) involves representing binary information with the charge configuration of closed cells comprised of several dots. Current does not flow between cells, but rather the Coulomb interaction between cells enables computation to occur. We use this system to explore, quantitatively and in a specific physical system, the relation between computation and energy dissipation. Our results support the connection made by Landauer between logical reversibility and physical reversibility. While computation always involves some energy dissipation, there is no fundamental lower limit on how much energy must be dissipated in performing a logically reversible computation. We explicitly calculate the amount of energy that is dissipated to the environment in both logically irreversible ''erase'' and logically reversible ''copy-then-erase'' operations carried out in finite time at nonzero temperature. The ''copy'' operation is performed by using a near-by QCA cell which plays the role of Maxwell's demon. The QCA shift register can then be viewed as a sequence of copy-then-erase operations where the role of the demon cell shifts down the line. © *2003 American Institute of Physics.* [DOI: 10.1063/1.1581350]

I. INTRODUCTION

From a technological perspective the question of the minimal amount of energy dissipation needed to accomplish computing is of increasing importance. As devices continue to shrink in size, power density will likely be the limiting factor for practical device densities. In developing a viable nanoscale computing technology, various approaches beyond complementary metal–oxide–semiconductor need to be evaluated in terms of functional density and power dissipation. This is of particular importance for technologies which use current to encode the information. A single electron passing through a 1 V potential to ground dissipates 1 eV of energy. At densities of 10^{12} devices/cm^2, a clock frequency of 1 THz, and using only a single electron to encode a bit, the resulting power dissipation is 160 kW/cm^2. A power dissipation rate of this magnitude simply melts the chip.

The question of minimal energy requirements in computation is connected to a larger discussion of entropy and the statistical interpretation of the second law of thermodynamics.[1] In 1875 Maxwell proposed a hypothetical creature which by measuring the state of a system could perform reversible processes on the system to reduce its entropy, and later this creature came to be known as Maxwell's demon. Szilard and more recently Brillouin proposed that the demon's apparent ability to circumvent the second law of thermodynamics did not take into account a minimal energy dissipation of $kT\ln(2)$ per bit which is associated with all measurement processes.[2,3] R. Landauer argued that it was not the act of measurement; but rather the irreversible erasure of the information produced by the measurement which requires a minimal energy dissipation of $kT\ln(2)$ per bit.[4] A result of Landauer's theory was that there is no fundamental energy dissipation limit associated with logically reversible computation. However, Landauer's argument was not a mathematical proof and relied on insight and intuition. It has not therefore gone uncontested. Frequently the discussion has been further confused by ambiguous terms like ''dissipationless computing'' and ''the amount of energy needed to compute a bit.''

In the context of this discussion it is instructive to quantitatively examine the role of energy dissipation, reversibility, and Maxwell's demon in a specific physical system. Here we choose as our system a set of clocked quantum-dot cellular automata (QCA) cells. An analysis of erasure in a model QCA system is performed to show that erasure can be accomplished with an arbitrarily small amount of dissipation provided that a copy of the bit is retained. We also show that much more energy is dissipated when a bit is erased without first undergoing the copy operation. Finally, in a specific QCA system, we make quantitative the phrase ''arbitrarily small amount of dissipation'' by explicitly calculating the amount of energy dissipated as a function of the length of time over which the erasure is performed. Our results are not a proof of Landauer's ideas, but rather a concrete demonstration of how energy and computation relate in a particular physical system.

We give an overview of the QCA concept in Sec. II. Section III introduces the coherence vector formalism used to describe dissipative dynamics in three-state QCA cells. In Sec. IV we employ this formalism to examine energetics in a single QCA cell for both logically reversible and irreversible bit erasure. The relevance of logically reversible bit erasure for the operation of a three-state QCA shift register is described in Sec. V.

II. QUANTUM-DOT CELLULAR AUTOMATA

The QCA concept[5] is an approach to binary computing at the nanoscale. A QCA cell is a structured charge container

a)Electronic mail: lent@nd.edu

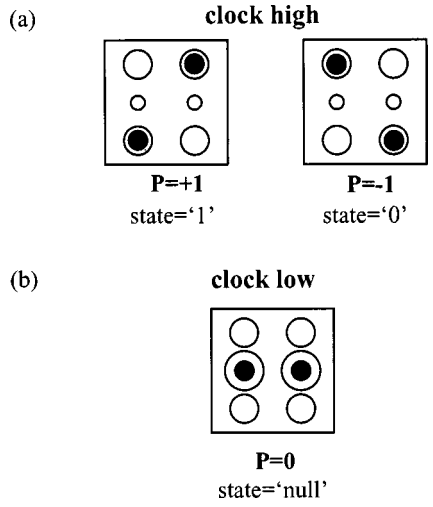

FIG. 1. Schematic of the six site QCS cell. (a) When the occupation energy of the middle dots is high, each electron is essentially localized to a single dot and Coulombic repulsion causes the electrons to occupy antipodal sites within the cell. The two resulting bistable states correspond to cell polarizations of $P=+1$ and $P=-1$. These polarizations have bit values 1 and 0, respectively. (b) When the occupation energy of the middle dots is low enough to ovecome the Coulombic repulsion of the electrons, the electrons occupy the middle dots. This configutation is designated the ''null'' state with $P=0$.

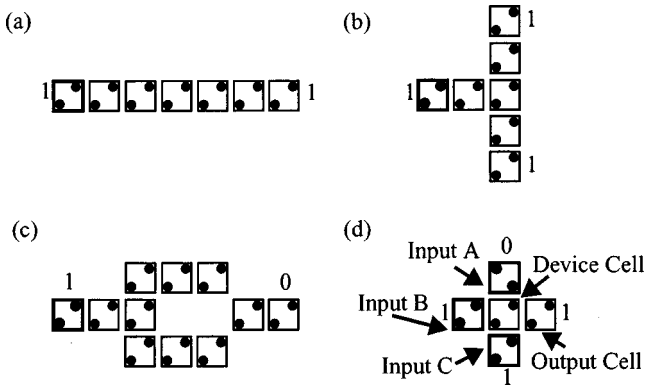

FIG. 2. Fundamental QCA devices. (a) The binary wire transmits data between two points (when clocked it functions as a shift register), (b) fanout provides a method to split a data signal and send the same value to two different destinations, (c) an inverter uses the Coulombic interaction of diagonally aligned cells to invert the input signal, and (d) the majority gate is the fundamental logical element of the QCA architecture where the output is the value corresponding to two or more of the three inputs.

where information is encoded in the charge configuration of the cell. The three charge configurations of a six-dot cell which correspond to logic states are schematically shown in Fig. 1. The ''dots'' are simply places an electron can occupy. The two polarized charge configurations of $P=1$ and $P=-1$ represent a binary ''1'' and ''0,'' respectively. The electrons can be pulled into the null state ($P=0$) by reducing the occupation energy of the central dots. Cell-to-cell interactions through which computation is accomplished are solely Coulombic. QCA computing is computing with the ground state which typically manifests itself as a natural tendency for a cell to align its polarization with its neighbors.

Clocked QCA cells facilitate the operation of large-scale circuits and minimize power dissipation. Cell configurations for binary wires, inverters, and the basic logic elements of the QCA architecture[6] are shown in Fig. 2. Clocking provides a means for controlling the flow of information through large arrays composed of these fundamental QCA elements.[7] A six-dot cell is clocked by changing the potential applied to the central dots. The clock pulls electrons into the middle dots or pushes them out by raising and lowering the occupation energies of the middle dots. A clocked switching event involves pulling the electrons from a polarized state into the null state and then pushing the electrons out of the null state into a new polarized state. Landauer and Keyes[8] first proposed this method of quasiadiabatic switching which has been adapted for use in six-dot cells. Gradual clocking maintains the cell arbitrarily close to its ground state throughout the switching process, so the adiabatic theorem[9] guarantees that if the switching is performed slowly enough it can be accomplished with an arbitrarily small amount of energy dissipation.

Working QCA logic devices have been successfully fabricated and tested.[10,11] These devices were made from cells comprised of metal dots connected by aluminum oxide tunnel junctions. Metal-dot cells are capacitively coupled and each dot contains many conduction band electrons. The high barriers in the tunnel junctions result in integer multiples of the elementary charge on each dot. In typical metal-dot cell operation, an applied voltage causes the transfer of a single electron from one dot to another and information is encoded in the charge configuration of the cell. Devices built from metal-dot cells include majority gates, latches, memories, and shift registers. Power gain has also been measured in experiments with metal dot cells.[12]

A molecular implementation of QCA holds the promise of approaching the ultimate limits in device densities, operating at room temperature, and achieving device switching speeds on the order of picoseconds.[13] In molecular QCA each cell is a single molecule. The dots in a QCA molecule are redox centers which are coupled by bridging ligands to provide tunneling paths between the dots.[14] Typical cell sizes are on the order of 1 nm. Cells do not need to be individually clocked, so molecular-scale cells could be clocked by wires with diameters of 10 nm or more.[15] Calculations show that clocked molecular cells exhibit power gain and are capable of operating at the ultralow power dissipation levels required for molecular scales of integration.[16] Full quantum-chemistry calculations have been performed on simple molecules to verify their switching behavior.[17] The fabrication and testing of single-molecule QCA cells is an area of active research.

As an approach to nanoscale computing, QCA avoids several of the difficult issue that confront conventional current-based methods and quantum computing. The problems associated with current at the nanoscale include the difficulty of charging the interconnect lines between devices with nanocurrents and the inability of a nanoscale current switch to cleanly turn the current off or on. The most significant problem is likely to be the high resistances and the even higher power dissipation associated with running current through molecular scale wires. If all other problems were somehow resolved and it was possible to fabricate a chip using current based devices at molecular scales of integra-

tion, the chip would simply melt as soon as it was turned on from the heat generated. QCA cells do not require charge transfer between devices and thus avoid the problems associated with current at the nanoscale. Neither do QCA cells require the full intercell quantum coherence necessary to perform analog quantum computing. The operation of a QCA cell requires tunneling, so switching does not occur if $\hbar$ is 0. Information, however, is only encoded in a cell's charge configuration which is a classical degree of freedom, so the interaction between neighboring cells need only be Coulombic in nature.[18]

III. THE DISSIPATIVE DYNAMICS OF A THREE-STATE QCA CELL

A three-state approximation provides a good model for a clocked QCA cell. The parameters of such a model can be deduced from more microscopic descriptions as shown in Ref. 19. In the three-state approximation, a QCA cell's Hamiltonian is constructed from basis vectors which correspond to the charge configurations of the three logic states. A basis vector is associated with the null state ($P=0$), and each of the two completely polarized states ($P=+1$ and $P=-1$). A cell's polarization in general is $P=-\langle\hat{\lambda}_7\rangle$, the projection of the cell's density matrix onto the seventh generator of SU(3)—see Appendix. Cell to cell interactions are characterized by the intercellular Hartree approximation[19] where Coulombic interaction between cells is treated with a mean-field approach, so any quantum entanglement between cells can be ignored. In Ref. 19 a quantitative comparison is made between the dynamics of a cell array under the mean-field approximation versus a description involving full quantum coherence.[20] The three state Hamiltonian for the jth cell of a QCA array is

$$\hat{H}_j=\begin{pmatrix} -\frac{E_k}{2}\sum_{m\neq j} f_{j,m}P_m & 0 & -\gamma \\ 0 & +\frac{E_k}{2}\sum_{m\neq j} f_{j,m}P_m & -\gamma \\ -\gamma & -\gamma & E_c \end{pmatrix}. \tag{1}$$

Here γ represents the tunneling energy between one of the symmetric polarization states [Fig. 1(a)] and the null state [Fig. 1(b)]. The symmetric off-diagonal zeros indicate that there is no direct coupling between the two symmetric polarization states, so the only tunneling path connecting them is through the null state. E_c is determined by the interaction of the cell's central dots with an external clocking field. The ''kink energy,'' E_k, is an energy which characterizes the Coulombic interaction between cells; E_k is the energetic cost of two neighboring cells having opposite polarizations. For molecular implementations this energy has been calculated to be greater than 0.5 eV. $P_m=-\langle\hat{\lambda}_7(m)\rangle$ is the polarization of the mth cell. The term $f_{j,m}$ is a geometric factor depending on the spatial relationship between the jth and the mth cells which can be calculated by simple application of electrostatics.

The ordered propagation of information through a QCA circuit is accomplished by clocking the cells. A four-phase clocking scheme was developed for a shift register composed of two-state molecular-scale cells in Ref. 16. The clocking there was accomplished by changing the tunneling energy between the dots. The three-state model has been developed to describe what appears to be a more practical way of effecting variations in the cells activity—directly altering the on-site energy of the central dots. This manner of clocking has been experimentally demonstrated in metal dot cells[11] where it is accomplished by simply adding gates to the central dots in the cell. That has the effect of altering the energy of the cell's ''null'' state. We model the clock simply as a controllable energy for this state, $E_c(t)$.

The terms used to describe the effects of the clock on a single cell are: null, active, locked, and erased. When the clock is low (E_c zero or negative), the electrons occupy the central dots and we say that the cell is in the null state, holding no information. As the clock signal is increased, the cell becomes ''active'' so the electrons are forced out of the central dots and the cell's polarization takes on a definite value determined by the neighboring polarizations. When the clock signal is large enough ($E_c \geqslant E_k$) to suppress switching over the relevant time scale, we say the cell is in the ''locked'' state. A locked cell can be in a metastable state where its polarization is independent of the environment. The locked cell is essentially a single-bit memory element. As the clock signal is decreased the cell depolarizes and any information stored in it is ''erased.''

Here we consider lines of equally spaced cells, so geometric effects can be absorbed into E_k and the Hamiltonian thus simplified to

$$\hat{H}_j=\begin{pmatrix} -\frac{E_k}{2}(P_{j-1}+P_{j+1}) & 0 & -\gamma \\ 0 & +\frac{E_k}{2}(P_{j-1}+P_{j+1}) & -\gamma \\ -\gamma & -\gamma & E_c \end{pmatrix}. \tag{2}$$

Only coupling to directly adjacent cells is considered in the earlier Hamiltonian because the interaction energy between cells, being a quadrupole–quadrupole interaction, decays as the fifth power of the distance.

We simulate the quantum dynamics of a three-state QCA cell using a coherence vector formalism where dissipative coupling to a heat bath is incorporated through an energy relaxation-time approximation. The coherence vector formalism (also called the generalized Bloch vector)[21] is developed by projecting the elements of the density matrix, $\hat{\rho}$, onto the generators of SU(3). The components of the coherence vector ($\vec{\lambda}$) are then

$$\lambda_i=\mathrm{Tr}\{\hat{\rho}\hat{\lambda}_i\}, \tag{3}$$

where $\hat{\lambda}_i$ is one of the generators of SU(3). In a similar fashion we project the three-state Hamiltonian onto the basis of generators to form a real eight-dimensional vector $\vec{\Gamma}$, the ''Hamiltonian,'' whose components are

$$\Gamma_i = \frac{\mathrm{Tr}\{\hat{H}\hat{\lambda}_i\}}{\hbar}. \tag{4}$$

The explicit form of the Hamiltonian vector corresponding to the Hamiltonian in Eq. (2) is

$$\vec{\Gamma} = \frac{1}{\hbar}\left[0, -2\gamma, -2\gamma, 0, 0, 0, E_k\overline{P}, \frac{2}{\sqrt{3}}E_c\right], \tag{5}$$

where $\overline{P}$ is simply the sum of the neighboring cell polarizations.

Without coupling to a heat bath, the equation of motion for the three-state coherence vector is

$$\frac{d}{dt}\vec{\lambda} = \Omega \cdot \vec{\lambda}. \tag{6}$$

The elements of the matrix Ω are

$$\Omega_{ik} = \sum_j \alpha_{ijk}\vec{\Gamma}_j, \tag{7}$$

where the structure constants α_{ijk} are determined by the commutator relation

$$\alpha_{ijk} = \frac{-i}{4}\mathrm{Tr}\{[\hat{\lambda}_i\hat{\lambda}_j] - \hat{\lambda}_k\}. \tag{8}$$

Equation (6) is completely equivalent to the quantum Liouville equation for the density matrix.

Dissipation is introduced into the coherence vector formalism through an energy relaxation time approximation where the system is relaxing to its instantaneous thermal equilibrium state. The instantaneous thermal equilibrium density matrix for a time-dependent Hamiltonian is

$$\hat{\rho}_{ss}(t) = \frac{e^{-\hat{H}(t)/k_BT}}{\mathrm{Tr}[e^{-\hat{H}(t)/k_BT}]}. \tag{9}$$

The components of the associated time dependent steady-state coherence vector are

$$\vec{\lambda}_{ss}^{(j)} = \mathrm{Tr}\{\hat{\rho}_{ss}(t)\hat{\lambda}_j\}. \tag{10}$$

The dissipative equation of motion can now be expressed as

$$\frac{\partial}{\partial t}\vec{\lambda} = \Omega \cdot \vec{\lambda} - \frac{1}{\tau}[\vec{\lambda} - \vec{\lambda}_{ss}(t)], \tag{11}$$

where τ is an energy relaxation time which represents the strength of the coupling between the system and the thermal bath. In addition to forcing terms, the dissipative equation of motion contains a term representing the system's tendency to relax to its instantaneous thermal equilibrium state.[22]

Energy flow through a QCA cell can be divided into terms each of which corresponds to a particular interaction of the cell with its surroundings. Specifically, a test cell exchanges energy with the clock, the bath, and its neighboring cells. We derive the energy flow terms from the instantaneous expectation value of the cell's energy which is

$$E = \langle\hat{H}\rangle = \frac{1}{3}\mathrm{Tr}\{\hat{H}\} + \frac{\hbar}{2}\vec{\Gamma}\cdot\vec{\lambda}. \tag{12}$$

By taking the derivative of Eq. (12) with respect to time, we obtain an equation for the instantaneous net power flow into the cell

$$P^f(t) = \frac{d}{dt}E = \frac{1}{3}\frac{d}{dt}E_c(t) + \frac{\hbar}{2}\left(\frac{d}{dt}\vec{\Gamma}(t)\cdot\vec{\lambda}(t) + \vec{\Gamma}(t)\cdot\frac{d}{dt}\vec{\lambda}(t)\right), \tag{13}$$

which after substituting Eq. (11) into the second term simplifies to

$$P^f(t) = \frac{1}{3}\frac{d}{dt}E_c(t) + \frac{\hbar}{2}\left(\frac{d}{dt}\vec{\Gamma}(t)\cdot\vec{\lambda}(t) - \frac{1}{\tau}\vec{\Gamma}(t)\cdot[\vec{\lambda}_{ss}(t) - \vec{\lambda}(t)]\right). \tag{14}$$

$\vec{\lambda}(t)$ evolves in time according to Eq. (11) and $\vec{\lambda}_{ss}(t)$ is the time dependent density matrix of Eq. (9) projected onto the generators of SU(3) per Eq. (10). The time dependence of a cell's Hamiltonian vector

$$\vec{\Gamma}(t) = \frac{1}{\hbar}\left[0, -2\gamma, -2\gamma, 0, 0, 0, E_k[P_L(t) + P_R(t)], \frac{2}{\sqrt{3}}E_c(t)\right] \tag{15}$$

depends on the clocking energy $E_c(t)$ and the polarization of the cells to the left $P_L(t)$ and right $P_R(t)$.

The total power flow through a cell averaged over a time interval T_s is

$$P^f = \frac{1}{T_s}\int_t^{t+T_s} P^f(t')dt', \tag{16}$$

and the net energy change over the same interval is

$$E_{\mathrm{net}} = \int_t^{t+T_s} P^f(t')dt'. \tag{17}$$

Using Eq. (14), we can write this as

$$E_{\mathrm{net}} = \int_t^{t+T_s}\frac{1}{3}\frac{d}{dt}E_c(t') + \frac{\hbar}{2}\left(\frac{d}{dt}\vec{\Gamma}(t')\cdot\vec{\lambda}(t') - \frac{1}{\tau}\vec{\Gamma}(t)\cdot[\vec{\lambda}_{ss}(t) - \vec{\lambda}(t)]\right)dt'. \tag{18}$$

The terms of Eq. (18) are identified with various components of the energy flow.

The energy transferred to the bath over time interval T_s is

$$E_{\mathrm{diss}} = \frac{\hbar}{2\tau}\int_t^{t+T_s}\vec{\Gamma}(t)\cdot[\vec{\lambda}_{ss}(t) - \vec{\lambda}(t)]dt'. \tag{19}$$

The energy delivered from the clock is

$$E_{\mathrm{clock}} = \frac{\hbar}{2}\int_t^{t+T_s}\frac{1}{3}\frac{d}{dt}E_c(t') + \frac{d\Gamma_8(t')}{dt'}\lambda_8(t')dt'. \tag{20}$$

The cell on the left of the test cell is the input cell. The energy it delivers to the test cell during interval T_s is

$$E_{\text{in}}=\frac{\hbar E_k}{2}\int_t^{t+T_s}\frac{dP_L(t')}{dt'}\lambda_7(t')dt'. \tag{21}$$

The cell on the right of the test cell is the output cell. The energy it receives from the test cell during interval T_s is

$$E_{\text{out}}=-\frac{\hbar E_k}{2}\int_t^{t+T_s}\frac{dP_R(t'}{dt'}\lambda_7(t')dt'. \tag{22}$$

With the sign conventions used in Eqs. (19)–(22) the net energy change of the cell over time interval T_s is

$$E_{\text{net}}=E_{\text{in}}-E_{\text{out}}+E_{\text{clock}}-E_{\text{diss}}. \tag{23}$$

The energy change in a cell for a given time period is not necessarily zero due to a cell's ability to store energy.

IV. THE THERMODYNAMICS OF BIT ERASURE

Bit erasure is the simplest logically irreversible process. It is logically irreversible in that it requires a one bit input and always returns the null state as the output, so it is impossible to recover the input value from just the output value. Other logically irreversible processes such as the one implemented by the majority gate involve a similar destruction of information about one or more of the inputs. While erasure is logically irreversible, the erasure of a bit in a specific cell can be transformed into a logically reversible process if a copy of the bit is made first. Landauer proposed a method for accomplishing logically reversible erasure in a bistable potential well provided that the erasure process was customized according to the value of the bit being erased.[4] In the context of QCA a similar process involving a demon cell (after Maxwell's demon) can be used to copy the bit stored in a cell and implement a logically reversible erasure process according to the value of the stored bit.

The focus of this section is to compare the energetics of two operations: ''erase bit'' and ''copy bit to demon, then erase bit.'' ''Erase'' is a process which returns a cell from a polarized state to the null state. Copying a bit to the demon involves allowing the physical interaction between the cell and the demon cell to set the demon cell into the same state as the cell. This can also be considered the demon cell ''reading'' the information in the primary cell; reading and copying are fundamentally the same operation. The role of the demon can be played by another cell or by any other read-out circuit, which stores a coy of the bit. We will show in Sec. V how a QCA shift register can be viewed as a series of copy-then-erase operations. The role of the demon then shifts from one cell to its neighbor as the copy of the bit propagates down the line.

The QCA testbed for single bit erasure consists of a driver, test cell, and demon cell (Fig. 3). The test cell's Hamiltonian vector $\hat{\Gamma}$, given by Eq. (5), changes with time in response to an external clocking field and the applied polarizations of the neighboring driver and demon cell. The summation of the drive and demon cell polarizations yields the value of P, and the strength of the external clocking field determines the value of E_c. The erasure process is described by the variation in time of $\hat{\Gamma}(t)$, and the corresponding response of the test cell is characterized by $\hat{\lambda}(t)$, evolving under the equation of motion [Eq. (11)]. The driver is assigned a polarization whose time dependence is structured to write a bit to the test cell. The operation of the demon cell is designed to assist in erasing the bit written to the test cell by the driver. The demon cell copies the test cell's polarization and then relaxes its polarization to zero which provides a path for the test cell to adiabatically reach its null state. Since operating the demon cell requires retaining a copy of the bit stored in the test cell, information is not destroyed and erasure assisted by the demon cell is logically reversible. Without the intervention of a demon cell, the erasure process is logically irreversible, as no copy of the bit is retained.

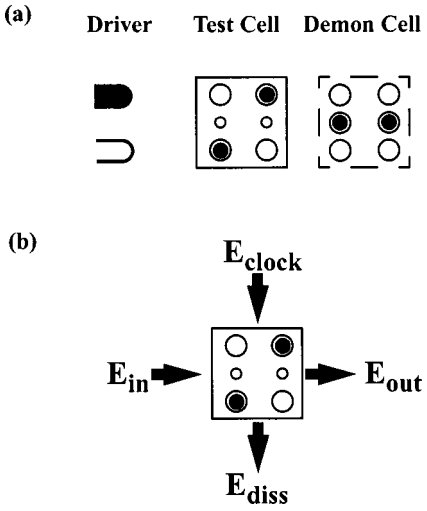

FIG. 3. QCA array for examining logically reversible and irreversible erasure. The driver writes the bit to the test cell. The test cell stores the bit written to it by the driver and is then erased with or without the assistance of the demon cell. The demon cell copies the test cell's polarization and drives the test cell to the null state, as it resets itself to the null state. If the demon cell is employed, it retains a copy of the bit value erased from the test cell. (b) Sign conventions for energy flow in a QCA cell. The arrow associated with each term indicates the direction of positive energy flow.

A. Bit erasure with no demon

Erasure without a demon cell is accomplished by lowering the clock, allowing the test cell to depolarize and the bit is erased. The logic values of a test cell undergoing erasure without a demon cell are shown in Fig. 4(a). Initially, a bit value of 1 is stored in the locked test cell. When the clock is lowered, dissipative effects erase the bit and the cell is left in the null state. Figure 5(a) gives the charge configurations for erasure without a demon cell. The test cell is initially locked with a polarization of 1 (the small central dots indicate that the cell is locked). The cell is unlocked by lowering the clock which decreases the occupation energy of the central dots (the large central dots indicate the cell is unlocked). Dissipative effects localize the electrons to the central dots and the cell is erased to a polarization of 0.

Figure 6 shows the dynamics of bit erasure without a demon cell. The dynamics are calculated from Eq. (11) by evolving the system forward from an initial state using an implicit time-matching method. The specific cell parameters and switching speed were chosen so that the characteristic dynamics of an irreversible erasure processes are easily ex-

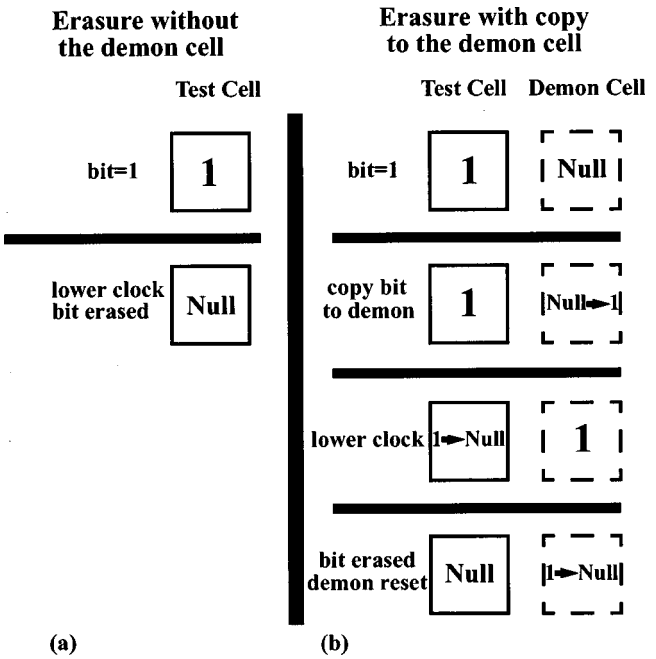

FIG. 4. Logical progression of bit erasure with and without a demon cell. (a) The column on the left shows the logic states of a test cell undergoing logically irreversible erasure without a demon cell. The test cell starts with a locked bit value of 1. The cell is unlocked by lowering the clock and the bit is erased by dissipative processes which relax the cell to the null state. (b) The column on the right shows the logical states of a test cell undergoing reversible erasure with the assistance of a demon cell. Again the test cell starts with a locked bit value of 1. The demon cell then copies the test cell's bit value. After the cell is unlocked by lowering the clock, the bit is quasiadiabatically erased as the test cell relaxes to the null state under the influence of the demon cell which drives it there.

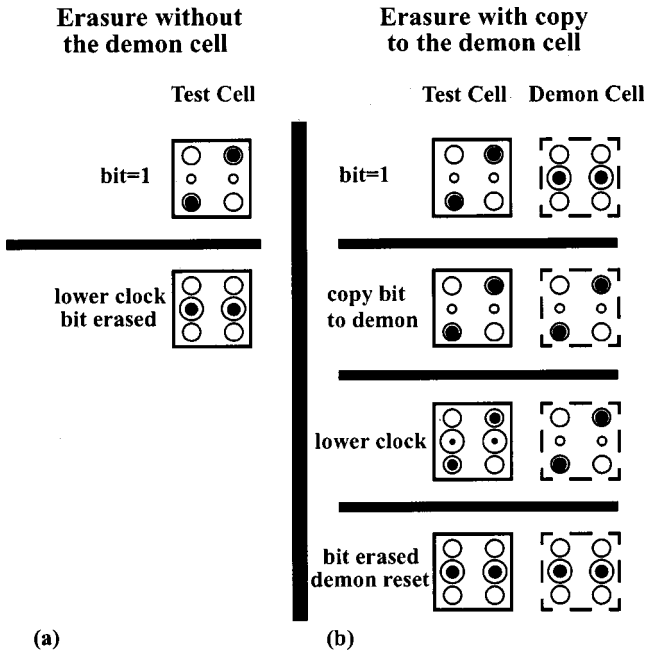

FIG. 5. Charge configurations for bit erasure with and without a demon cell. (a) The column on the left shows the charge configuration of a test cell undergoing logically irreversible erasure without a demon cell. The test cell starts with a locked polarization of 1 where the small central dots indicate the cell is locked. The cell is unlocked by lowering the clock which is indicated by the large central dots. Lowering the clock decreases the occupation energy of the central dots. The electrons are then localized to the central dots through dissipative processes, and the bit value formerly encoded in the cell's charge configuration is irreversibly erased. (b) The column on the right shows the charge configurations of a test cell undergoing logically reversible erasure with the assistance of a demon cell. Again the test cell starts with a locked polarization of 1. The demon cell then copies the test cell's bit value and adopts its polarization. Next the test cell is unlocked by lowering the clock, it remains polarized due to the influence of the demon cell. Finally, the test cell is erased when the demon cell resets to a polarization of 0 and drives the test cell adiabatically to the null state. This process is logically reversible, since the demon cell retains a copy of the bit erased from the test cell and could be used to write the bit back onto the test cell.

hibited ($E_k/kT=20$, $\gamma=0.1$, E_k, $\tau=100\ \hbar/\gamma$). The driver and test cell initially have polarizations of zero and the test cell's clock is low. A bit is written to the test cell, and then the bit is erased according to the logically irreversible process outlined in Fig. 4. The labeled time intervals of Fig. 6 are explained in the following step by step outline of the logically irreversible erasure process (the transitions of the clock, driver, and demon cell are all error-function-shaped in time).

(1) Write bit. The driver's polarization goes from 0 to 1. The test cell copies the driver's polarization.
(2) Lock bit. The clock signal is increased. The test cell is locked and fully polarized.
(3) Store bit. The driver's polarization goes from 1 back to 0. The test cell remains locked with a polarization of 1 due to the influence of the clock.
(4) Erase bit. The clock signal is decreased. The test cell is unlocked and it is erased as dissipative effects drive its polarization to 0.

Since the test cell is coupled to an external heat bath, even in its locked state it will begin to depolarize as energy escapes to the bath. The energy relaxation time constant τ determines the rate at which a locked cell will depolarize. When the clock is lowered, the unlocked cell completely depolarizes on a time scale much shorter than τ. After the clock is lowered and the bit erased, the kinetic energy trapped in the cell escapes to the thermal bath and the Rabi oscillations are damped by dissipative processes.

B. Bit erasure with a copy to demon

Bit erasure with a demon cell is a logically reversible copy-then-erase process. The logic values of a copy-then-erase process for a test cell and a demon cell are shown in Fig. 4(b). Initially, a bit value of 1 is stored in the locked test cell and the demon cell is in the null state. First, the demon cell copies the bit value of 1 stored in the test cell. Next the test cell's clock is lowered, but the cell partially retains a bit value of 1 due to the influence of the demon cell. Finally, the demon cell is reset to the null state which allows the test cell to fully depolarize and the bit is erased.

The charge configurations for a copy-then-erase process are shown in Fig. 4(b). The test cell starts with a locked polarization of 1. First the demon cell copies the test cell's polarization. The second step is that the test cell is unlocked by lowering the clock, but it remains almost fully polarized

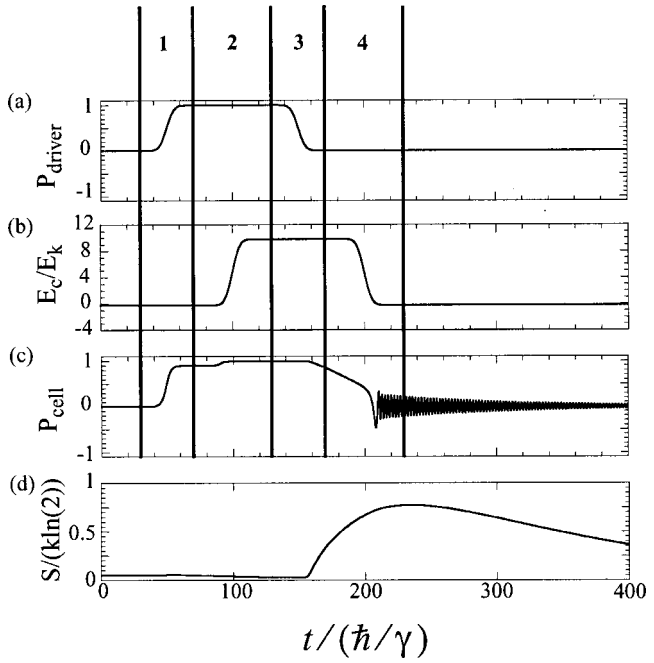

FIG. 6. Calculated dynamics of a logically irreversible erasure process. (a) The time dependent polarization of the driver cell as it writes a bit to the test cell. (b) The clock signal applied to the test cell which is increased to lock the bit written by the driver and then decreased allowing dissipative processes to irreversibly erase the bit. (c) Polarization of the test cell, as it responds to the effects of the driver and the clock. The test cell becomes fully polarized as the bit is written to it and then the clock is lowered and dissipative effects erase the test cell. (d) There is a significant increase in the test cell's entropy as the bit is irreversibly erased. The numbered time intervals 1–4 indicate the following steps in the logically irreversible erasure process: 1 write bit, 2 lock bit, 3 store bit, and 4 erase bit.

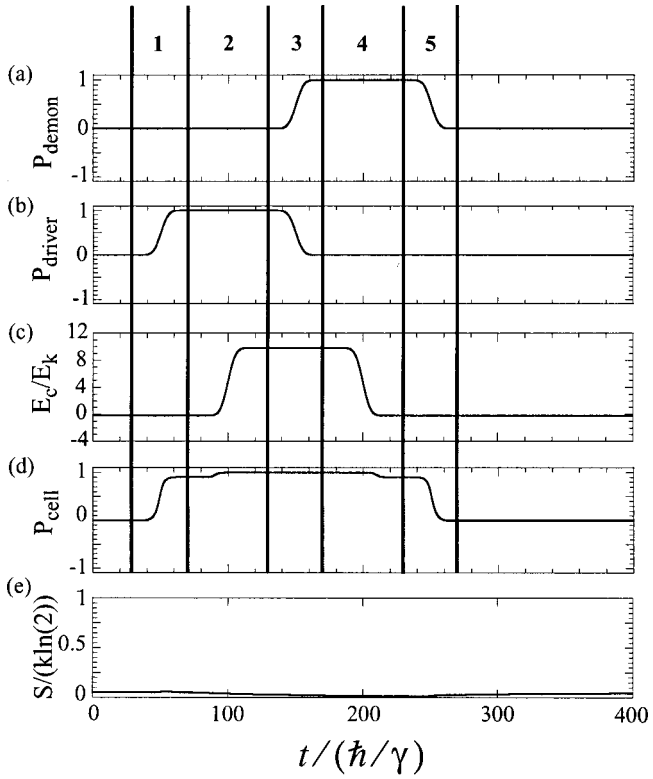

FIG. 7. Calculated dynamics of a logically reversible erasure process. (a) The time dependent polarization of the demon cell as it copies the polarization of the test cell and then erases the test cell to the null stat.e (b) The polarization of the driver cell as it writes a bit to the test cell. (c) The clock signal applied to the test cell which is increased to lock the bit written by the driver and then decreased to allow the demon cell to reversibly erase the bit. (d) Polarization of the test cell, as it responds to the effects of the driver, clock, and demon cell. The test cell becomes polarized as the bit is written and then adiabatically resets to the null state under the influence of the demon cell. (e) No entropy is generated during the reversible erasure process. The numbered time intervals 1–5 indicate the following steps in the logically reversible erasure process: 1 write bit, 2 lock bit, 3 copy stored bit, 4 unlock bit, and 5 erase bit.

due to the influence of the demon cell. Finally, the test cell is erased when the demon cell resets its polarization to 0 and drives the test cell to the null state.

Figure 7 shows the dynamics of a copy-then-erase process with a demon cell. The dynamics are calculated using the same methods described for logically irreversible erasure and the same cell parameters are used. The driver and test cell initially have polarizations of zero and the test cell's clock is low. A bit is written to the test cell, and then the bit is erased according to the logically reversible copy-then-erase process outlined in Fig. 4(b). The labeled time intervals of Fig. 7 are explained in the following step by step outline of the logically reversible erasure process.

(1) Write bit. The driver's polarization goes from 0 to 1. The test cell copies the driver's polarization.
(2) Lock bit. The clock signal is increased. The test cell is locked and fully polarized.
(3) Copy stored bit. The driver's polarization goes from 1 back to 0. The demon cell's polarization goes from 0 to 1, as it copies the polarization of the test cell. The test cell remains locked with a polarization of 1 due to the influence of the clock and demon cell.
(4) Unlock bit. The clock signal is decreased. The test cell is unlocked but it remains almost fully polarized due to the influence of the demon cell.
(5) Erase bit. The demon cell resets to a polarization of 0. The test cell is erased to a polarization of 0 as the demon cell resets.

C. Entropy

It is instructive to examine the entropy during the operations. We use von Neumann's definition which, expressed in terms of the density matrix is

$$S = -kTr\{\rho \ln \rho\}. \tag{24}$$

For the erasure events shown in Figs. 6 and 7 the time-dependent density matrix is reconstructed from the test cell's coherence vector and the entropy calculated from Eq. (24). Entropy is generated only in the case of logically irreversible erasure without a demon cell [shown in Fig. 6(d)]. The entropy generated in the erasure process then flows out into the environment. During a copy-then-erase process [shown in Fig. 7(e)], by contrast, the entropy is nearly constant at the thermal equilibrium value. In fact, the clock acts to briefly refrigerate the cell and entropy temporarily decreases.

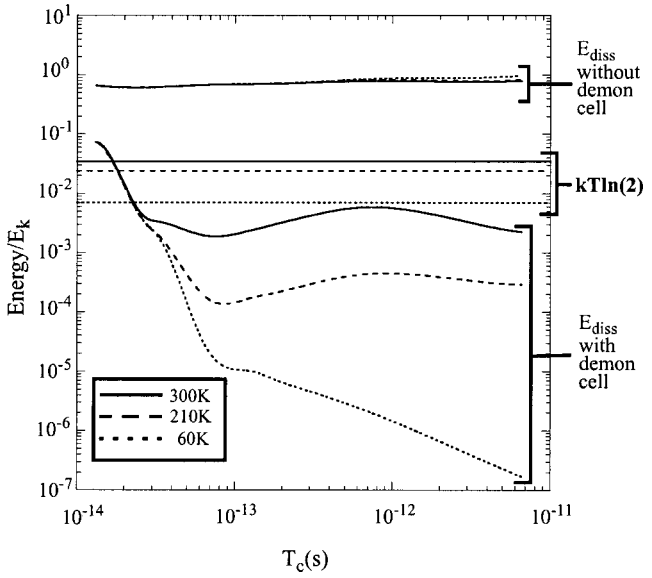

FIG. 8. The energy dissipated to the bath by the test cell for logically irreversible and reversible erasure processes. For a particular erasure event, T_c is the time interval over which the clock energy E_c goes from high to low. There are three groups of curves plotted as a function of T_c. The set of curves grouped under $kT\ln(2)$ designate the minimum signal energy required to reliably distinguish a bit from the thermal bath at various temperatures. The curves grouped under E_{diss} without demon cell are the calculated values of the energy dissipated to the environment for logically irreversible erasure events of the type shown in Fig. 6. The curves labeled E_{diss} with demon cell are the calculated values of the energy dissipated to the environment for logically reversible copy-then-erase processes of the type shown in Fig. 7. Here we see that for a copy-then-erase process the energy dissipated to the environment can be significantly smaller than $kT\ln(2)$, while for logically irreversible erasure the energy dissipated is on the order of E_k.

D. Minimum energy dissipation requirements for computation

We calculate the energy dissipated during the erasure and copy-then-erase processes. It is important to distinguish signal energy, which is the energy associated with the transfer of information between cells (i.e., the work one cell does on the succeeding cell), from energy dissipated to the environment. Erasure without a demon cell typically requires an amount of energy to be dissipated on the order of the signal energy. However, the copy-then-erase process does not require any minimum amount of energy to be dissipated, subject to the requirement of slowing the process down. That is, if a copy of the information is retained, the energy dissipated in erasing a bit from a cell can be made arbitrarily small, provided the erasure time is sufficiently long.

We quantify the relationship between erasure time and energy dissipation. For the erasure and copy-then-erase procedures described in the preceding subsections A and B, we calculate the energy dissipated to the bath using Eq. (19) for a test cell with the following characteristics: $E_k = 0.52$ eV, $\gamma = 0.1\ E_k$, and $\tau = 10\,000\ \hbar/E_k$. Figure 8 shows the energy dissipated to the bath during erasure in a test cell as a function of the time interval, T_s, over which the erasure was performed. In this case T_s is defined as the time interval over which the clock energy E_c goes from high to low. The graph contains three groups of curves and each group contains data for temperatures of 60, 210, and 300 K. The values of $kT\ln(2)$ for each of these temperatures are shown. The set of curves labeled "E_{diss} without demon cell" correspond to irreversible erasure events (Fig. 6), in which the amount of energy dissipated to the environment is always considerably larger than $kT\ln(2)$. The set of curves labeled E_{diss} with demon cell correspond to copy-then-erase processes (Fig. 7) where the amount of energy dissipated can be significantly less than the $kT\ln(2)$ limit. This set of curves shows quantitatively that in the case of logically reversible computation, energy dissipation is a design issue and not a fundamental physical limit.

V. A DEMON CHAIN—THE QCA SHIFT REGISTER

QCA shift registers are linear arrays of cells which directionally propagate binary information encoded in the charge configurations of the component cells. One of their primary functions in the QCA architecture is to transport data between logic elements. Adiabatic switching of a QCA shift register was first discussed in Ref. 23, developed in detail for metal-dot cells in Ref. 24, and demonstrated experimentally for metal-dot cells in Ref. 11. QCA shift registers also exhibit power gain,[16] which has been experimentally verified in metal-dot cells.[12] The initial considerations of such a shift register go back to Landauer's work on fundamental limits for computation[8] and communication.[25]

We focus on the shift register as we can use it to examine the steady-state behavior of many QCA cells involved in a series of write, copy, and erase operations. In steady state the net transferred into the cell over a clock cycle, E_{net} in Eq. (23), must be zero. The shift register allows us to focus on steady-state energy balance, rather than on transient behavior.

We consider a QCA shift register with a four-phase clocking scheme in which each cell's individual clock is delayed a quarter period from that of the previous cell. In actual molecular implementations the clock signal would be distributed over a larger length scale than just individual cells. Many molecules of single-nanometer dimensions could be clocked by one clock wire with dimensions on the order of tens of nanometers, and the cell arrays could process as well as transport information.[23] We adopt the single-clock-per cell model for simplicity.

The clocking scheme is shown in detail in Fig. 9. Clock signal 2 is a quarter period behind clock signal 1 [T_c is the clock period and $E_c^{(j)}$ is the clocking energy of the jth cell]. This quarter period delay allows a locked cell to polarize its active downstream neighbor without any back influence from the following cell downstream, because the latter is held in the null state. After the bit in a locked cell is copied to its active neighbor, the locked cell is erased and the down stream cell formerly in the active state becomes locked. In this manner every quarter clock period the bit moves one cell down the chain (Fig. 10).

The calculated polarizations of a semi-infinite QCA shift register with three state cells is shown in Fig. 11. The shift register is capable of propagating an arbitrary bit stream. Each cell's dynamics are determined by Eq. (11) and the cell-to-cell coupling, as well as the cell-to-driver coupling, is

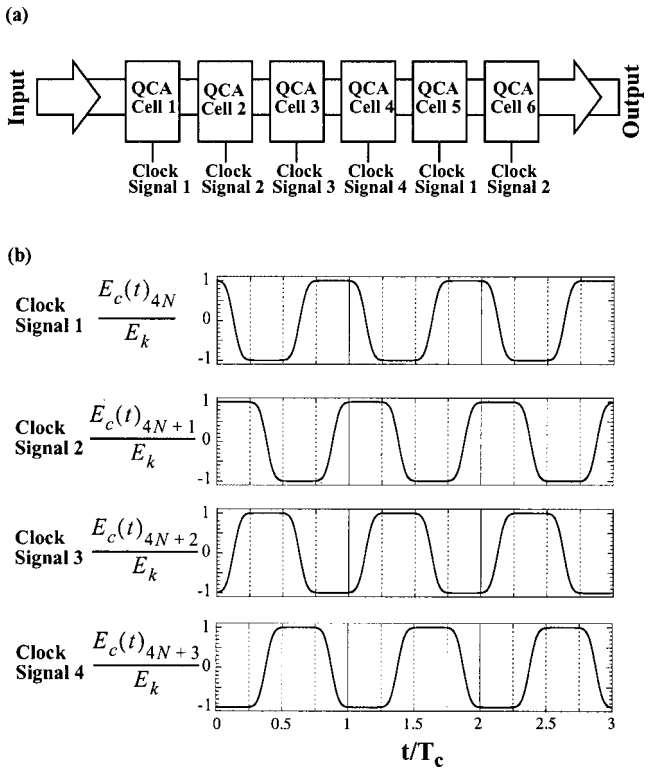

FIG. 9. Schematic of a QCA shift register with a four phase clocking scheme. The data advances one cell to the right with each quarter clock cycle. (b) The four clock signals which order the propagation of data through the shift register. The quarter clock cycle phase delay allows a locked cell to polarize its active downstream neighbor which will in turn become locked during the next quarter clock cycle and polarize its active downstream neighbor.

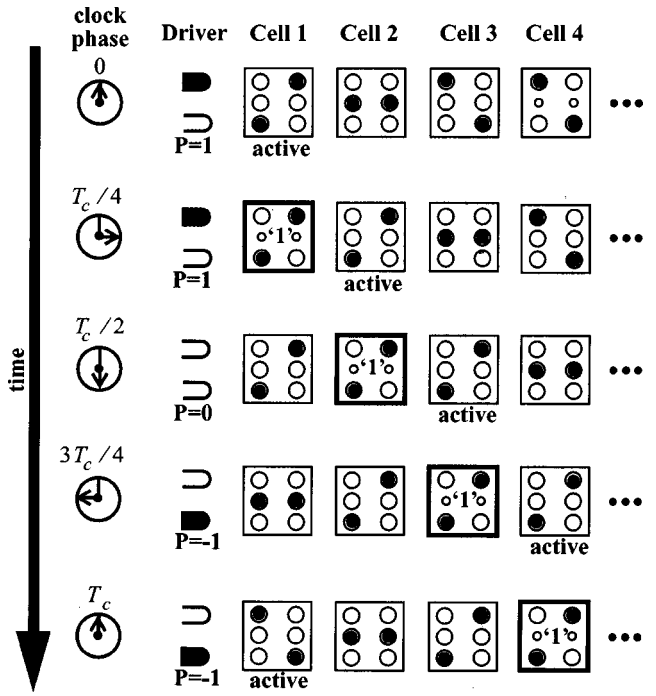

FIG. 10. Data propagation in a QCA shift register over one clock cycle. The cells in the process of copying a bit are labeled active. Locked cells storing a bit have bold outlines and are labeled with the bit value they contain which in this case is "1." Each descending row corresponds to the clock signals advancing a quarter cycle which causes the bit in the locked cell to be transferred to its active downstream neighbor. The net result is that the bit written by the driver to cell 1 in the first row advances four cells over the course of a complete clock cycle.

treated using the mean-field approximation discussed earlier. Implicit time marching is used to evolve the coupled system forward in time. For the shift register simulation shown the relevant three state parameters are: $E_k=0.2$ eV, $\gamma=0.2\,E_k$, maximum $E_c=E_k$, minimum $E_c=-E_k$, $T_c=5$ ps, $T=300$ K, $\tau=10\,\hbar/E_k$ (they are again chosen to make the behavior readily apparent). Figure 11 shows both bit values of 0 and 1 propagating from the driver to the demon cell.

Every cell in a QCA shift register plays the role of a demon cell for part of the time. The characteristics of a demon cell are that it copies the bit from a neighboring cell and that it uses the stored bit value to adiabatically reset the neighboring cell to the null state. In the active state, a cell is copying the bit value of its upstream neighbor. In the locked state a cell stores the copied bit value in its charge configuration thereby maintaining the correct polarization bias for adiabatically erasing the upstream neighbor. Because the operation of copy-then-erase is logically reversible, the energy dissipated to the thermal bath per switching event can be much less than $kT\ln(2)$.

We perform a quantitative analysis of energy flow through a three-state QCA shift register. The components of the energy flow through a QCA cell over one switching cycle in a shift register under steady-state conditions are shown in Fig. 12. In this case steady-state means transients associated with clocking information into a shift register initially at thermal equilibrium have decayed and the behavior of the shift register is periodic with the clock period T_c. With the cell parameters from the shift register of Fig. 11, we use Eq. (11) to calculate the cell's dynamics. The energy flow values over one clock cycle are then calculated from Eqs. (19)–(22). Under steady-state conditions the energy which flows into a cell when the upstream cell writs a bit to it, E_{in}, is equal to the energy delivered to the downstream cell when the bit is erased, E_{out}. During the process of writing and erasing the bit an amount of energy, E_{diss}, which is significantly less than $kT\ln(2)$, is dissipated to the bath, and replaced by an equivalent amount of energy from the clock, E_{clock}. A signal energy much greater than $kT\ln(2)$ is transferred to the downstream cell when it copies a bit. This energy is not dissipated and must be significantly greater than $kT\ln(2)$ to preserve the integrity of the information encoded in the signal from the disruptive effects of the thermal bath. The signal energy is only necessarily dissipated to the bath in the case of a logically irreversible erasure where the information in the signal is destroyed without being copied. In that case the energy dissipated is much more than $kT\ln(2)$ (see E_{diss} without demon cell in Fig. 8). Note that the equivalence of E_{diss} and E_{clock} are results of the calculated time-marching behavior, not *a priori* assumptions.

The energy dissipated per switch as a function of clock frequency is shown in Fig. 13 for a cell in a QCA shift register under steady-state operation. The upper bound of the QCA operation region is based on irreversible switching events where the cell's operation is completely nonadiabatic, the information the cell contained may have been erased in a

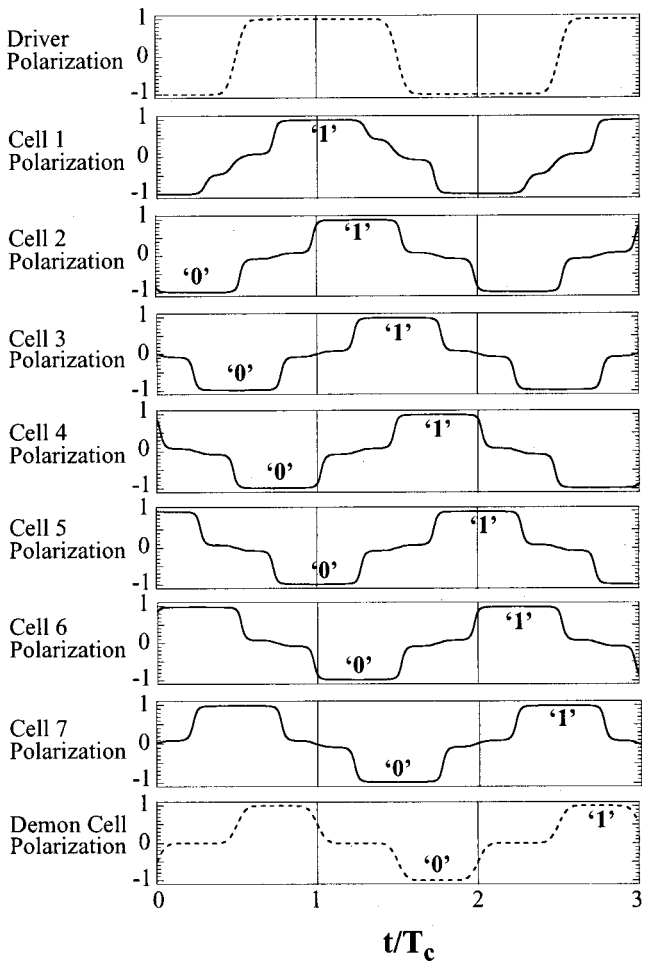

FIG. 11. Semi-infinite QCA shift register composed of three state cells. The polarization of each cell is calculated from a self-consistne time-marching solution of Eq. (11). The initiawl transition of the driver cell's polarization from -1 to 1 (bit value 0 to 1) propagates down the cell chain, as does each subsequent transition. The demon cell at the end of the chain simulates the response of the next cell in a semi-infinite line. The labels "1" and "0" show the propagation of two bits down the shift register. In this case T_c is 5 ps.

logically irreversible manner, and an amount of energy on the order of E_k must be dissipated during each switching event. The lower bound corresponds to quasiadiabatic logically reversible switching events in which the information in the cell is copied before being erased. In the case of the lower bound, an arbitrarily small amount of energy can be dissipated at the price of decreasing the clock frequency. The physical parameters of the cells used to calculate the points defining the lower limit of the QCA operation region are: $E_k=0.1$ eV, $\gamma=0.2\ E_k$, maximum $E_c=E_k$, minimum $E_c=-E_k$, $T=300$ K, and $\tau=1000\ \hbar/E_k$. These parameters were chosen to give a conservative estimate of the QCA operation region with respect to energy dissipation. Even using nonoptimal parameters a large portion of the QCA operation region is comprised of switching events which, at room temperature, dissipate less than the thermal background energy. From a technological perspective it is noteworthy that the room temperature QCA operation region indicates cells could operate at tetrahertz speeds with power dissipation rates of 10 pW or less[26] (point A in Fig. 13).

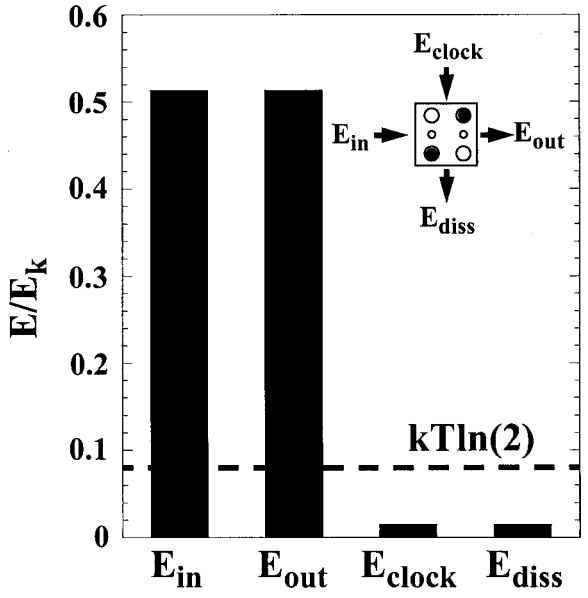

FIG. 12. Steady-state energy flow in a QCA shift register. Over one clock cycle a bit is written to the cell, copied by the next cell downstream, and reversibly erased. The signal energy corresponding to the bit is delivered by the upstream cell (E_{in}) and sent to the downstream cell (E_{out}). The signal energy is much greater than $kT\ln(2)$ so that the information encoded in the signal is not corrupted by the thermal environment. The energy dissipated to the bath (E_{diss}) over the course of a clock cycle is much less than $kT\ln(2)$. Still this would result in degradation of the signal energy, if it were not replaced by energy from the clock signal (E_{clock}).

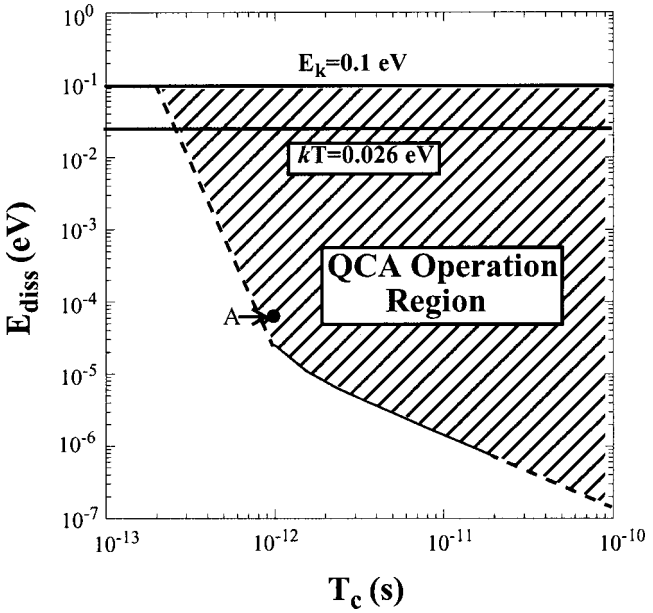

FIG. 13. The QCA operation region gives the energy dissipated to the environment per cell as a function of the clock period (T_c). The upper bound of the region corresponds to an abruptly switching cell which dissipates an amount of energy corresponding to the value of its kink energy over every clock cycle (in this case $E_k=100$ meV). The solid line in the lower bound corresponds to the same cell switching quasiadiabatically at 300 K with weak coupling to the environment. Point A is a reference point that indicates the amount of energy dissipated per switching event by a cell with a clock frequency of 1 THz and a power dissipation of 10 pW.

VI. CONCLUSION

We have examined the energetics of a simple QCA array which included dissipative coupling to a thermal bath. The primary focus has been to quantitatively assess the energy dissipated in logically reversible and irreversible processes in this particular physical system, and connect these results to the broader question of the minimum energy required to perform computing.

Our analysis supports the connection made by Landauer[4,8,27] between two conceptually distinguishable concepts: logical reversibility and physical reversibility. While any computation done in a physical system must dissipate energy to the environment, a logically reversible operation, like copy-then-erase, can be executed with as little energy dissipation as desired, at the cost of performing the operation slowly. We have calculated quantitatively just how much energy is dissipated in such operation performed in a QCA system. Importantly, the copy operation does require the transfer of information between QCA cells, and the amount of energy transferred must be greater than $kT\ln(2)$ per bit. But that signal energy is not lost to the environment and could in principle be recovered and reused. For a logically irreversible process like erase, an energy comparable to the signal energy, and therefore larger than $kT\ln(2)$ must be dissipated to the environment. The QCA shift register (which we note has been fabricated in metal tunnel junctions) also stands as a specific example of Landauer's contention[27] that there is no fundamental minimum energy-dissipation required to communicate a bit. We have not presented a proof; but rather specific examples in a concrete computational system with potential technological relevance.

ACKNOWLEDGMENTS

This work was supported by the Office of Naval Research MURI program.

APPENDIX: GENERATORS OF SU(3)

The coherence vector formalism is developed by projecting the operators of the density matrix formalism on the generators of SU(3). Of special importance are the generators $\hat{\lambda}_7$ and $\hat{\lambda}_8$ which correspond to a system's classical degrees of freedom. The polarization is defined as

$$P = -\mathrm{Tr}\{\hat{\lambda}_7\hat{\rho}\}. \tag{A1}$$

The other observable corresponding to a classical degree of freedom is called the activity which is defined as

$$A = \mathrm{Tr}\{\hat{\lambda}_8\hat{\rho}\}. \tag{A2}$$

Polarization measures the dipole moment of a cell due to its charge configuration. Activity measures how much charge is localized in the central dots versus the top and bottom dots. The rest of the SU(3) generators correspond to quantum degrees of freedom. Here is a complete list of the SU(3) generators which are traceless and Hermitian by definition

$$\hat{\lambda}_1 = \begin{bmatrix} 0 & 1 & 0 \\ 1 & 0 & 0 \\ 0 & 0 & 0 \end{bmatrix} \quad \hat{\lambda}_2 = \begin{bmatrix} 0 & 0 & 1 \\ 0 & 0 & 0 \\ 1 & 0 & 0 \end{bmatrix} \quad \hat{\lambda}_3 \begin{bmatrix} 0 & 0 & 0 \\ 0 & 0 & 1 \\ 0 & 1 & 0 \end{bmatrix}$$

$$\hat{\lambda}_4 = \begin{bmatrix} 0 & i & 0 \\ -i & 0 & 0 \\ 0 & 0 & 0 \end{bmatrix} \quad \hat{\lambda}_5 = \begin{bmatrix} 0 & 0 & i \\ 0 & 0 & 0 \\ -i & 0 & 0 \end{bmatrix}$$

$$\hat{\lambda}_6 = \begin{bmatrix} 0 & 0 & 0 \\ 0 & 0 & i \\ 0 & -i & 0 \end{bmatrix} \quad \hat{\lambda}_7 = \begin{bmatrix} -1 & 0 & 0 \\ 0 & 1 & 0 \\ 0 & 0 & 0 \end{bmatrix}$$

$$\hat{\lambda}_8 = \frac{1}{\sqrt{3}} \begin{bmatrix} -1 & 0 & 0 \\ 0 & -1 & 0 \\ 0 & 0 & 2 \end{bmatrix}. \tag{A3}$$

[1] H. Leff and A. Rex, *Maxwell's Demon: Entropy, Information, Computing* (Princeton University Press, Princeton, NJ, 1990). An excellent compilation of the significant contributions to the discussion of entropy and information processing.
[2] L. Szilard, Behav. Sci. **9**, 301 (1964).
[3] L. Brillouin, J. Appl. Phys. **22**, 334 (1951).
[4] R. Landauer, IBM J. Res. Dev. **5**, 183 (1961).
[5] C. S. Lent, P. D. Tougaw, and W. Porod, Appl. Phys. Lett. **62**, 714 (1993); C. S. Lent, P. D. Tougaw, W. Porod, and G. H. Bernstein, Nanotechnology **4**, 49 (1993).
[6] P. D. Tougaw and C. S. Lent, "Logical devices implemented using quantum cellular automata," J. Appl. Phys. **75**, 1818–1825 (1994).
[7] M. Niemier and P. M. Kogge, Int. Conf. on Electronics, Circuits and Systems (ICECS '99), Cyprus, Sept. 1999.
[8] R. Landauer and R. W. Keyes, IBM J. Res. Dev. **14**, 2 (1970).
[9] D.J. Griffiths, *Introduction to Quantum Mechanics* (Prentice Hall, Englewood Cliffs, NJ, 1994).
[10] C. S. Lent and P. D. Tougaw, J. Appl. Phys. **75**, 4077 (1994); G. Toth and C. S. Lent, *ibid.* **85**, 2977 (1999); A. O. Orlov, I. Amlani, G. H. Bernstein, C. S. Lent, and G. L. Snider, Science (Washington, DC, U.S.) **277**, 928 (1997); I. Amlani, A. Orlov, G. Toth, G. H. Bernstein, C. S. Lent, and G. L. Snider, *ibid.* **284**, 289 (1999).
[11] A. O. Orlov, I. Amlani, R. Kummamuru, R. Rajagopal, G. Toth, C. S. Lent, G. H. Bernstein, and G. L. Snider, Appl. Phys. Lett. **77**, 295 (2000); A. O. Orlov, R. Kummamuru, R. Ramasubramaniam, G. Toth, C. S. Lent, G. H. Bernstein, and G. L. Snider, *ibid.* **78**, 1625 (2001).
[12] R. Kummamuru, J. Timler, G. Toth, C. S. Lent, R. Ramasubramaniam, A. O. Orlov, G. H. Bernstein, and G. L. Snider, Appl. Phys. Lett. **81**, 1332 (2002).
[13] C. S. Lent, Science (Washington, DC, U.S.) **288**, 1597 (2000).
[14] M. Lieberman, S. Chellamma, B. Varughese, Y. Wang, C. S. Lent, G. H. Bernstein, G. L. Snider, and F. C. Peiris, Ann. N.Y. Acad. Sci. **960**, 225 (2002).
[15] K. Hennessy and C. S. Lent, J. Vac. Sci. Technol. B **19**, 1752 (2001).
[16] J. Timler and C. S. Lent, J. Appl. Phys. **91**, 823 (2002).
[17] C. S. Lent, B. Isaacson, and M. Lieberman, J. Am. Chem. Soc. **125**, 1056 (2003).
[18] The QCA concept can be extended to the quantum-computing regime. See G. Toth and C. S. Lent, Phys. Rev. A **63**, 052315 (2001).
[19] P. D. Tougaw and C. S. Lent, J. Appl. Phys. **80**, 4722 (1996).
[20] The Hartree approximation is sufficient for modeling the quasiadiabatic dynamics considered here.
[21] G. Mahler and V. A. Weberruß, *Quantum Networks: Dynamics of Open Nanostructures* (Springer, New York, 1995).
[22] The corresponding equation of motion in terms of the density matrix is a modified form of the Lindblad master equation, $(\partial/\partial t)\hat{\rho} = -i/\hbar[\hat{H},\hat{\rho}] - (1/\tau)(\hat{\rho}-\hat{\rho}_{ss})$.
[23] C. S. Lent and P. D. Tougaw, Proc. IEEE **85**, 541 (1997).
[24] G. Toth and C. S. Lent, J. Appl. Phys. **85**, 2977 (1999).
[25] R. Landauer, Appl. Phys. Lett. **51**, 2056 (1987).
[26] At 10 pW per device a chip area of 1 cm with a device density of 10^{13} devices/cm^2 has a net power dissipation of 100 W.
[27] R. Landauer, Phys. Rev. Lett. **53**, 1205 (1984).